EPJ AP

Applied Physics

EPJ.org
your physics journal

Eur. Phys. J. Appl. Phys. **49**, 11001 (2010) DOI: 10.1051/epjap/2009181

Analysis of positive corona in wire-to-plate electrostatic precipitator

H. Nouri and Y. Zebboudj

EDP SCIENCES

The title "The European Physical Journal" is a joint property of EDP Sciences, Società Italiana di Fisica (SIF) and Springer

Eur. Phys. J. Appl. Phys. **49**, 11001 (2010)
DOI: 10.1051/epjap/2009181

THE EUROPEAN PHYSICAL JOURNAL APPLIED PHYSICS

Regular Article

Analysis of positive corona in wire-to-plate electrostatic precipitator

H. Nouri and Y. Zebboudj[a]

Laboratoire de Génie Électrique, Université A. Mira de Béjaïa, 06000 Béjaïa, Algeria

Received: 15 September 2008 / Received in final form: 24 April 2009 / Accepted: 21 September 2009
Published online: 26 November 2009 –

Abstract. This paper analyses corona discharge in ambient air flow associated with laboratory-scaled wire-to-plate electrostatic precipitator (WPESP). The corona discharge is analysed by a combined iterative computational technique based on the finite element method (FEM) and charge simulation method (CSM). The phenomenon is mathematically described by Maxwell's equations in differential form. A finite element method is used to solve the Poisson's equation and the charge simulation method is used to satisfy the current continuity condition. Measurement method of the positive dc corona current density and electric field, taking into account the air flow velocity, has been introduced. The computed results are compared with experimental results to test the effectiveness of this approach.

PACS. 51.50.+v Electrical properties (ionization, breakdown, electron and ion mobility, etc.) – 52.70.-m Plasma diagnostic techniques and instrumentation – 52.80.-s Electric discharges

1 Introduction

Electrostatic precipitators are used to collect suspended particles in gases using an electrostatic force and they are the one ways to control air pollution caused by industrial plants. The configuration mostly used in electrostatic precipitation technique is the wires-to-plates. It consists of high-field parallel active wires located midway between the grounded plates (the collecting electrodes) where the air flows through. The ions produced by the corona discharge near the wires charge the dust particles which are thus driven toward the collecting plates. The particle charges are neutralised and the particle is thus collected. The collection efficiency of the wire-to-plate electrostatic precipitators (WPESPs) depends on numerous variables like the global drift velocity of charged particles to be removed and their distributions, the magnitude of applied voltage, the active electrodes radius, the humidity and temperature of the air, etc.

The basic corona discharge physics is well-known and it can be described as a self-sustaining electrical gas discharge occurring at the vicinity of high-field electrodes. In the WPESPs the high-field wires are surrounded by ionisation region where the free charges are produced and a low-field drift region where charged particles drift to the collecting plates. The corona drift region is governed by the Poisson's equation and the current continuity equation. A complete solution of these equations is not straightforward. For practical applications, therefore, empirical and semi-empirical formulas have a useful function.

When the number of wires is high the geometry can be considered equivalent to a coaxial system as described by Cooperman [1], where the equivalent cylinder radius R_e is given by:

$$R_e = \frac{a}{2\pi} e^{\frac{\pi h}{a}} \tag{1}$$

and the inception field E_i according to the inception voltage V_i at the wires surface is given by:

$$E_i = \frac{V_i}{R \ln \frac{R_e}{R}}, \tag{2}$$

where h is the wires-to-plate spacing, a is the half wire-to-wire spacing and R is the wires radius. The Cooperman's model is widely used in the design and evaluation of precipitators.

In this paper we have proposed a numerical method to solve the Poisson's equation and a method to measure the electric field at the one grounded plates where the velocity of the air flow through the grounded plates is associated. The method uses the finite-element and the current continuity equation which updates the space charge density using the simplified method of characteristics.

The space charge modifies the original Laplacian applied field and the measurements of this field over the collector electrode are not easy in presence of space charge.

[a] e-mail: yzebboudj@yahoo.fr

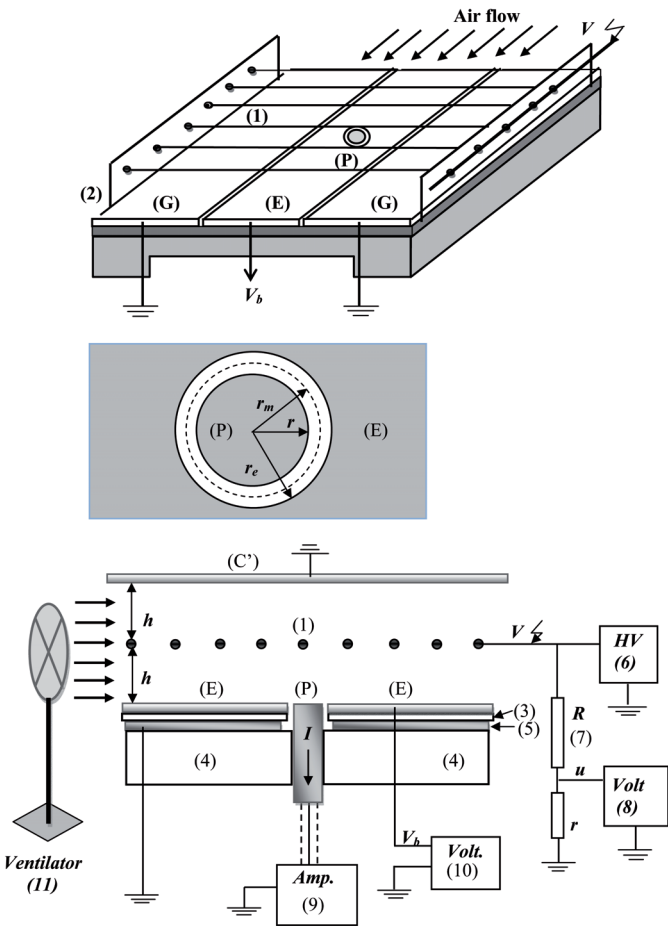

Fig. 1. Experimental assembly with the circular field probe (not in scale). 1: corona wires; 2, 3, 4: insulating props; 5: screen; 6: dc high voltage source; 7: high voltage divider; 8: voltmeter; 9: picoammeter; 10: dc low voltage source. P probe collector; E biased electrode; G guard planes; C' collector plane.

The introduced method of electric field measurement uses the Tassicker's biased probes [2–5] which are simple circular or linear sensors, incorporated on a same level of surface in a plane electrode biased at a voltage. They can be miniaturised and suitable for dc corona discharge.

2 Experimental apparatus and design of the probe system

The experimental method aims to obtain new measurements of current density and electric field for positive dc corona in laboratory-scaled WPESP, Figure 1, and in which the velocity of the ambient air flow, free of all particles, is controlled. 13 parallel wires (1) are fixed with two insulating supports (2) and located midway between two planes (C) and (C') at $h = 50$ mm and the wire-to-wire spacing is fixed at $a = 40$ mm, where (C) is made up of one biased electrode (E), a circular probe (P) and two guard planes (G). The probe is incorporated on a same level of surface at the centre of the electrode (E) and the end-effects were prevented by the two guard planes (G). All the components are made of stainless steel and are fixed with insulating props. Positive direct voltage, supplied by a $0-\pm 140$ kV source (6), is applied to the wires, a high voltage divider (7) and a dc voltmeter (8) are used to measure the applied voltage V. The current probe collector (P) is connected to a picoammeter (9) and the plane is online to the dc low voltage source (10). The larger of the polarised plate (E) is $l = 200$ mm according to the z-axis and the longer is $L = 800$ mm according to the x-axis.

The air flow along the x-axis is generated by a ventilator (11) online to an ac low voltage source and the velocity v is measured by means of an anemometer. The system is calibrated in absence of the discharge in measuring v with varying the supplied source voltage U and the characteristic $v - U$ is thus used for the velocity control when the corona discharge occurs in the WPESP. The ventilator allows to follow continuously the air across the precipitator and we can to vary the velocity of the flow.

The probe requires a careful assembly. Indeed, some leakage current, of about a few pico-ampers could result from the bias plate (E) or the high voltage wires and affecting the current measurements. The probe is fixed with two insulating plates (4) and the leakage was prevented by using a screen (5). The leakage current between the corona wires and the probe is evacuated to earth by the guard planes (G).

The circular biased probe theory is fully developed in [2,3], but will be briefly recalled in this section. The probe collector (P) collects a current I_0 resulting from the corona discharge. This current will be reduced or increased to I when a voltage V_b is applied to the plate (E) in producing a bias electric field E_b. In fact, E_b is opposed to the unknown field E at the surface of the probe collector (P) when $V_b < 0$ and E_b is added to E when $V_b > 0$. The corona currents I under the condition V_b and I_0 under the condition $V_b = 0$ are respectively:

$$I = JS = \mu\rho\,(E + E_b)\,S = \mu\rho\left(\frac{\varphi_{S0} + \varphi_{S1}}{\varepsilon_0}\right) \quad (3)$$

$$I_0 = J_0 S = \mu\rho E S = \mu\rho\frac{\varphi_{S0}}{\varepsilon_0}\cdot \quad (4)$$

μ is the positive ion mobility ($\mathrm{m^2/V\,s}$), ρ the space charge density ($\mathrm{C/m^3}$), $S = \pi r_m^2$ ($\mathrm{m^2}$) is the effective surface of the collector (P), r_m is the effective radius, φ_{S0} is the flux due to the unknown electric field E to be measured and φ_{S1} is the flux due to the biased electric field E_b:

$$\varphi_{S0} = SE\varepsilon_0 \quad (5)$$

$$\varphi_{S1} = C_0 V_b. \quad (6)$$

C_0 is the capacity between the probe collector (P) and the polarised plate (E) [6]

$$C_0 = 4r\varepsilon_0\left[1.07944 + 0.5\ln\left(1 + \frac{r}{2g}\right)\right]. \quad (7)$$

Where r is the radius of the collector (P) and g the air gap between (P) and (E).

From equations (3)–(6) the current ration is given by:

$$\frac{I}{I_0} = 1 + \frac{C_0}{\pi\varepsilon_0 r_m^2}\frac{V_b}{E}. \quad (8)$$

The unknown external field E could be determined by the measurements of I_0 and I. The relationship (8) gives a characteristic I/I_0 linear with the biased voltage V_b. However, for high values of V_b, when the total field at the surface of the plate is inverted, due to the polarised electric field $E_b > E$, a deviation of the characteristics occurs and thus the relationship (8) is not valid.

The probe functions depend mainly on the choice of these dimensions and the precision of its construction. A good sensitivity of the current ratio I/I_0 is obtained for a probe radius r not very high and an air gap g very small. The ratio r/g must be as high as reasonably possible. The probe must be easily removable for a regular cleaning from dust. The model under consideration is optimised to obtain these qualities. The probe collector radius is $r = 2.235$ mm, the plate orifice is $r_e = 2.27$ mm, which gives an air gap $g = 0.035$ mm, a ratio $r/g = 64$, an effective radius of the probe collector $r_m = r + g/2 = 2.2525$ mm and the capacity value $C_0 = 0.223$ pF.

The expression (8) can be written as:

$$\frac{I}{I_0} = 1 + PV_b \quad (9)$$

with

$$P = \frac{C_0}{\pi\varepsilon_0 r_m^2 E} = \frac{1585.35}{E}. \quad (10)$$

The slope P is determined by the measurements of the current ratio I/I_0 and the polarised voltage V_b, thus, the electric field E can be determined if P is known.

To verify probe function, we used 13 polished wires of radius $R = 0.200$ mm. We made the measurements of I/I_0 for different bias voltages V_b, between –100 and +100 V, where the corona voltage V and the air velocity v are maintained constant during the tests. The measurements have allowed us to determine the field E, at the plate surface, using equations (9) and (10). The current ration I/I_0 values measured for various applied corona voltage are shown in Figure 2. In all the cases, the characteristic $I/I_0 = f(V_b)$ is linear for -80 V $< V_b <$ $+80$ V. The deviation of the characteristics occurs when $V_b > 80$ V or $V_b < -80$ V. These results provide a verification of the probe function and the limit of the polarisation voltage V_b.

The inception corona voltage V_i is deduced from the measurements of the dc corona current-voltage characteristics and the method is fully described in [7]. Tests with our laboratory-scaled WPESP were made in air with varying the number n of wires and the results are shown in Figure 3 for positive and negative corona discharge. The measured inception voltage V_i according to the number n of discharging wires remained constant for $n > 5$ and equal to 12.0 kV for positive corona and 12.8 kV for negative corona. This result confirms the predicted Cooperman's theory [1] widely used in the WPESPs.

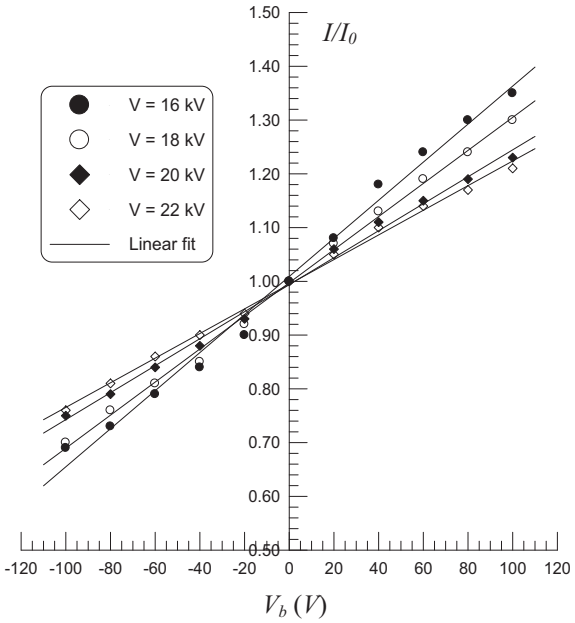

Fig. 2. Measured current density ration I/I_0 as a function of the bias voltage V_b.

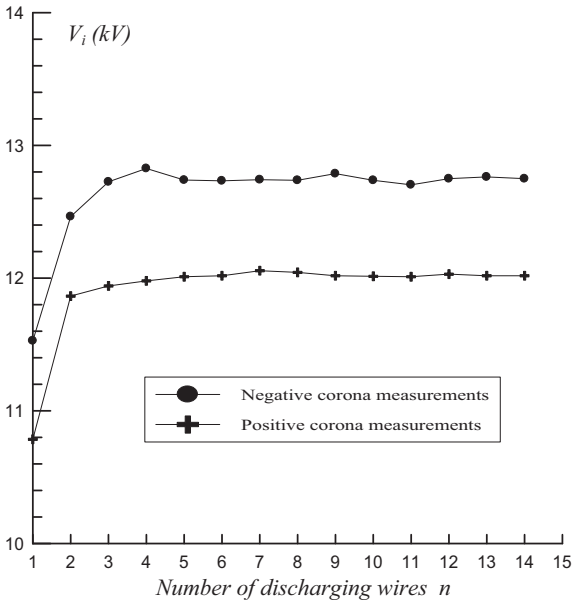

Fig. 3. Measured inception corona voltage versus the number of discharging wires.

3 Boundary conditions and numerical computation

The method uses the finite-element and the current continuity equation which updates the space charge density using the simplified method of characteristics. The velocity of the ions under the effect of the electric field and the air flow is higher than the velocity of their diffusion. The ion diffusion is thus neglected for a small distance between electrodes and the ion mobility under the electric field is

taken as constant. These assumptions are largely used in the literature [8–11].

The system of equations that constitute the mathematical description of the corona is:

$$\vec{\nabla}\vec{E} = \frac{\rho}{\varepsilon_0} \tag{11}$$

$$\vec{\nabla}\vec{J} = 0 \tag{12}$$

$$\vec{J} = \rho\left(\mu\vec{E} + \vec{v}\right) \tag{13}$$

$$\vec{E} = -\vec{\nabla}\Phi. \tag{14}$$

Where $\vec{E}$ is the vector electric field (V/m), Φ the electric potential (V), $\vec{J}$ the current density vector (A/m^2), μ the positive ion mobility (m^2/V s), ε_0 the air permittivity (F/m), ρ the space charge density (C/m^3) and $\vec{v}$ the velocity vector of the air flow (m/s).

Actually, it is difficult to find an exact solution to equations (11)–(14) because of their non linear nature, for this, many attempts have been made for describing corona discharge. Simplifying approaches have been developed for these basic equations to formulate theoretical models for descriptions of charge density and electric field distributions in the wire-to-plane and coaxial systems. Deutsch's assumption [12] stipulates that the space charge affects only the magnitude and not the direction of the electric field. This assumption is commonly accepted in analytical approaches in the past, it is satisfied in coaxial cylindrical configuration but in wire-to-plane system it is not verified. Kaptzov's assumption postulates that the electric field distribution at the wire remains constant whatever is the applied voltage [13]. The ionisation layer thickness around the wires is always disregarded with respect to the interelectrode space. The space between electrodes is characterised mainly by the transport of positive ions.

This paper describes an iterative finite element technique proposed as a numerical tool to solve Poisson's equation in using new boundary conditions for the electric field in WPESP. The Deutsch's assumption is overlooked here. The boundary conditions are developed in [7] where the corona is subdivided in two distinct regions, the ionisation and the drift regions:

- The ionisation region, $R < r < R_c$, is considered of circular form because its thickness layer is small. It is separated from the drift region by a boundary of radius R_c. In this region, it is often assumed to the first order, that the electric field is described adequately by Laplace's equation. That is, within this region, the space charge field is assumed to be dominated by the geometric electric field associated with the large curvature of the wire.
- The drift region, $R_c < r < h$, is characterised mainly by the transport of positive ions to the grounded planes and within this region the electric field is significantly distorted by space charge. It is often assumed that, to the first order, the space charge is formed by positive ions.

The electric field E_c, at the ionisation region/drift region (IRDR) interface corresponds to a zero net ionisation coefficient ($\alpha - \eta = 0$). The minimum ionisation field E_c is calculated by Hartmann [14] from a representation of $(\alpha - \eta)/P = f(E/P, H_a)$ for the range $0 < E/P < 750$ V/cm mbar. The computed results are expressed by an analytic equation:

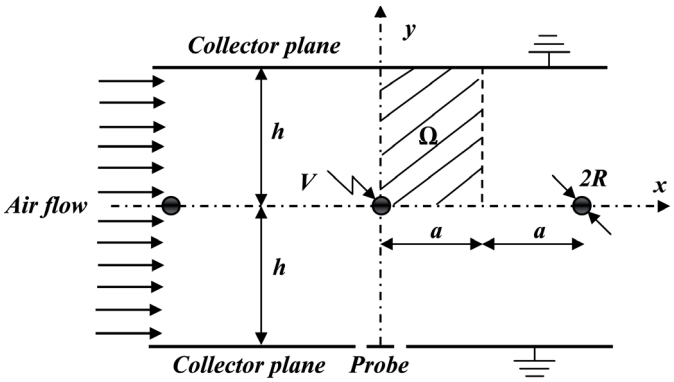

Fig. 4. Computational domain with borders.

$$E_c\left(\delta, H_a\right) = E_c(1,0)\delta\left(1 + \alpha_h\sqrt{H_a}\right) \tag{15}$$

with

$$\delta = \frac{P}{1013}\,\frac{293}{273+T}. \tag{16}$$

δ is the related air density ($\delta = 1$ for $P = 1013$ mbar and $T = 20$ °C) and H_a is the absolute humidity in g/m^3. $E_c(1,0) = 2.468 \times 10^6$ V/m and $\alpha_h = 1.603 \times 10^{-2}$ (g/m^3)$^{-1/2}$.

The average mobility of positive ions is often assumed to be constant during the transit time from the ionisation region to the collecting planes. It is also considered to be independent of the electric field. Indeed, in ambient air at atmospheric pressure, the variations of the reduced field are insignificant in the drift region.

The field equations are solved in WPESP taking into account the layer of the ionisation region. We neglected here Deutsch's assumption and diffusion of ions. The new boundary condition proposed is the IRDR interface where $r = R_c$ and $E(R_c) = E_c$. The corona radius is easily found from the Kaptzov's assumption which stipulates that the field at the surface of the corona wires remains at the inception value E_i. If the space charge field of the ionisation region is ignored, then R_c is given by the relationship:

$$R_c = \frac{E_i}{E_c}R. \tag{17}$$

The computational domain can be reduced to the rectangular Ω of dimensions $h \times a$, as shown in Figure 4, due to the double symmetry in the WPESP geometry and the boundary conditions $E_x = 0$ along the symmetry line y-axis and $E_y = 0$ along the symmetry line x-axis are indirectly satisfied. To solve equations (11)–(14), the following boundary conditions are required:

(i) The potential of the corona wires is equal to the applied voltage ($\Phi = V$);

(ii) The potential of the grounded plates is zero ($\Phi = 0$);
(iii) The initial charge density value at the IRDR interface ($r = R_c$) is given in [15,16]:

$$\rho_{R_c,j} = \rho_e \cos\left(\frac{\theta_j}{2}\right) \qquad j = 1, 2, 3, \ldots, n\,, \tag{18}$$

where j is related to the field line number and θ is the angle formed by the jth field line and the y-axis and ρ_e is given by:

$$\rho_e = \rho_0 \frac{h}{R_e} \frac{E_0}{E_i} \tag{19}$$

$$\rho_0 = \frac{4\pi_0 V_i \left(V - V_i\right)}{h^2 V \left(5 - 4\frac{V_i}{V}\right)} \tag{20}$$

$$E_0 = \frac{V_i}{h \ln \frac{R_e}{R}}, \tag{21}$$

where V_i is the corona inception voltage and E_0 is the field at the plane surface.

In the present investigation the WPESP is supposed to be infinite length and consequently the system is reduced to 2D. Under the condition of double symmetry, one fourth of the cross-section area Ω of rectangular form is enough for the problem formulation, Figure 4. The method of analysis is described in the following steps:

Step 1. The first grid generation is mapped in the absence of the space charge density, and therefore the electric field is due to the applied voltage. We used the charge simulation method to map the space charge free lines. Once the field lines are drawn, we connect the points of the same potential on all field lines. The node (i, j) represents the intersection between the jth field line and the ith equipotential contour. The linear triangular elements are obtained by subdividing each quadrangle produced by the intersection of field lines and equipotentials contours into two triangles.

Step 2. Solve for Φ the Laplace's equation via the finite element technique (assuming $\rho = 0$ in the entire domain). The estimation of the electric field values E is done using the interpolation/extrapolation method.

Step 3. Estimate the space charge density on the border of the ionisation region by using equation (18).

Step 4. The evaluation of the space charge density for the other grid nodes is gotten while using the method of characteristics which taken into account the air velocity and neglected ion diffusion. Thus, from equations (11)–(13) we can write:

$$\vec{\nabla}\left[\rho\left(\mu\vec{E} + \vec{v}\right)\right] = 0 \Rightarrow \left(\mu\vec{E} + \vec{v}\right)\vec{\nabla}\rho + \rho\vec{\nabla}\left(\mu\vec{E} + \vec{v}\right) = \left(\mu\vec{E} + \vec{v}\right)\vec{\nabla}\rho + \rho\mu\frac{\rho}{\varepsilon_0} = 0. \tag{22}$$

Equation (22) can be written as:

$$\vec{\nabla}\rho = -\frac{\rho^2}{\varepsilon_0\left(\vec{E} + \frac{\vec{v}}{\mu}\right)}. \tag{23}$$

Along field lines, equation (23) becomes:

$$\frac{\partial\rho}{\partial r} = -\frac{\rho^2}{\varepsilon_0\left(\vec{E} + \frac{\vec{v}}{\mu}\right)}. \tag{24}$$

Integration of equation (24) gives the values of the space charge density along field lines. As initial values of E we took those gotten in step 2 and for the resolution of equation (24), we used the modified method of Euler.

Step 5. Solve the Poisson's equation via the finite element method.

$$\Delta\Phi + \frac{\rho}{\varepsilon_0} = 0. \tag{25}$$

Step 6. Calculate the electric field distribution from the potential interpolation. These values will be used for the revaluation of the space charge density on the grid nodes.

Step 7. Repeat steps 4–6 until the maximum mismatch (E_{rr}) between the last two estimates of the potential at each node, Φ^l and Φ^{l+1}, is less than a pre-specified error δ_1. E_{rr} is defined as:

$$E_{rr} = \frac{\left|\Phi^{(l)} - \Phi^{(l+1)}\right|}{\Phi_{av}} \tag{26}$$

with $\Phi = \frac{(\Phi^{(l)} - \Phi^{(l+1)})}{2}$ and l is the iteration number.

Step 8. Estimate discrete charges $q(i)$. They are given as follows:

$$q(i) = \rho(i)_{moy}\Delta_e(i) \tag{27}$$

with

$$\rho(i)_{moy} = \left(\frac{\rho(1) + \rho(2) + \rho(3)}{3}\right). \tag{28}$$

$\rho(1)$, $\rho(2)$ and $\rho(3)$ are the space charge density values on the ith triangle peak, which area is $\Delta_e(i)$.

Step 9. Reconstruct the orthogonal grid. Discrete charges estimated in step 8 modify the Laplacian electrostatic field and distorts field lines. Indeed, the electrostatic field in any grid point is the superposition of fields created by all charges including the ones simulating the electrodes system. These last charges will be modified to keep the same applied voltage on the wires. Once the space charge is estimated on all the nodes of the grid, the Poisson's equation can be solved using the finite element method and in which our contribution appears when we introduced the new third boundary condition: the potential corresponding to the minimum ionisation field ($E = E_c$ for $\alpha - \eta = 0$). This condition speeds up the numerical resolution since it eliminates the loop of convergence for the electric field at the border of the ionisation region. Once the Poisson's equation is solved, the density of the space charge is restored until the distribution of the potential reaches a stable value. Thus, the discrete space charges are localised in the centres of the triangular elements. This will again allow the reconstitution of the electrostatic grid in the presence of the space charge. To keep the potential on the wires equal to the applied voltage, we must reappraise the value of the charge on the wires taking account

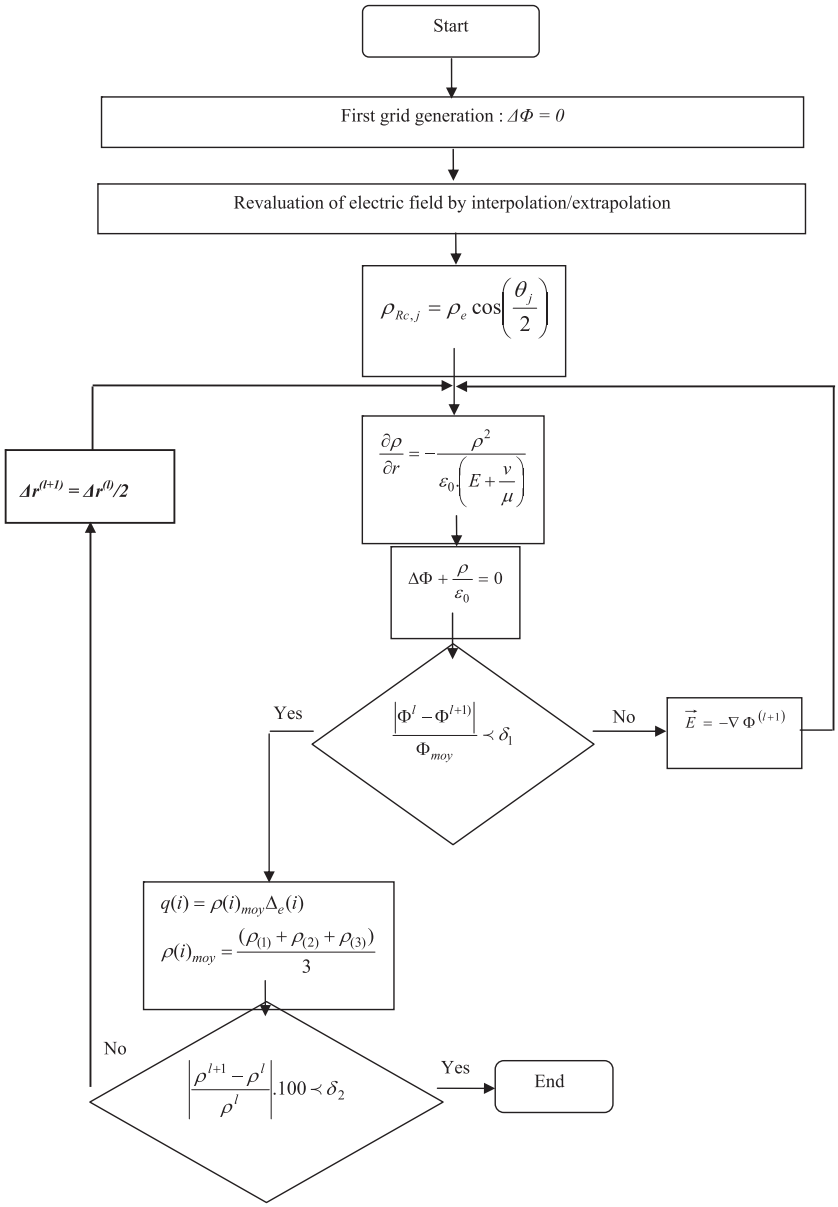

Fig. 5. Flow-**c**hart of the numerical procedure.

of all the discrete charges and then do all the preceding steps until the stability of the electrostatic grid.

Step 10. Steps 3–9 are repeated until the difference value between the space charge densities of two consecutive grids is less than a pre-specified value δ_2.

Figure 5 shows the flow-chart that describes these steps of analysis.

4 Results and discussion

The method of analysis is applied to the corona discharge in our laboratory-scaled WPESP. The air flow, free of all particles, is provided with a ventilator where the velocity is controlled. The ion mobility μ is taken as constant in the drift region. This assumption is commonly used and has been experimentally confirmed for the positive ions [16] and the value of μ is taken equal to 2×10^{-4} m^2/V s. The probe collector is also used to measure the normal current density J_n when the probe is unbiased ($V_b = 0$):

$$J_n = \frac{I_0}{\pi r_m^2}. \tag{29}$$

Where $r_m = 2.25$ mm is the effective radius of the probe and I_0 the collected current of corona discharge. The current density given by equation (13) can be written as the sum of a normal component due to the electric field E and a tangential component due to the air flow velocity v:

$$\vec{J} = \vec{J_n} + \vec{J_t} \tag{30}$$

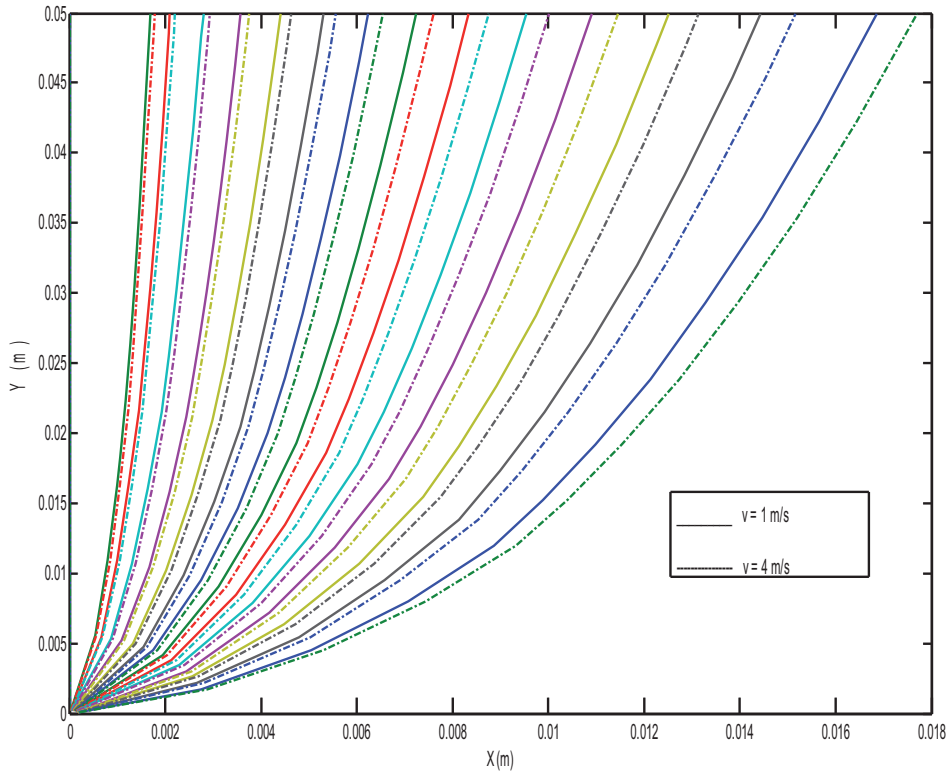

Fig. 6. (Color online) Electric field lines in the computed domain Ω (corona wires radius $R = 0.200$ mm, applied voltage $V = 20$ kV, air flow velocity: $v = 1$ m/s for continue line and $v = 4$ m/s for dashed line).

with

$$\vec{J_n} = \rho\mu\vec{E} \tag{31}$$

and

$$\vec{J_t} = \rho\vec{v}. \tag{32}$$

The charge density can be thus deduced at the plane surface from equation (31):

$$\rho = \frac{J_n}{\mu E}. \tag{33}$$

The electric field lines in the computed domain are shown in Figure 6 for two values of the air flow velocity. The deflection of the field lines indicate that the charges are deflected in the direction of the air flow. The electric field strength E, the current density J and the charge density ρ at the probe collector according to the air flow velocity v and for various corona applied voltage V are shown respectively in Figures 7–9. It can be seen that the present calculated values of the J, E and ρ fit reasonably the measured ones and increased weakly with v. In the laboratory-scaled WPESP for the number of wires $n = 1$ and where the probe collector is fixed at the centre of the plane collector beneath the wire ($x = 0$) the values of J, E and ρ are maximum for $x = 0$ and they decrease as we move away from the centre of this plane along the x-axis according to the Warburg's law [5]. For $n = 13$ J, E and ρ are maximum beneath the wires and minimum at midway between the wires according to the superimposing principle. The characteristics $J(x)$ $E(x)$ and $\rho(x)$ are deflected by the air flow along the x-axis which causes the weak increasing of the values of J, E and ρ. In fact the probe collector (P) is 8 mm moved forward the centre during the tests.

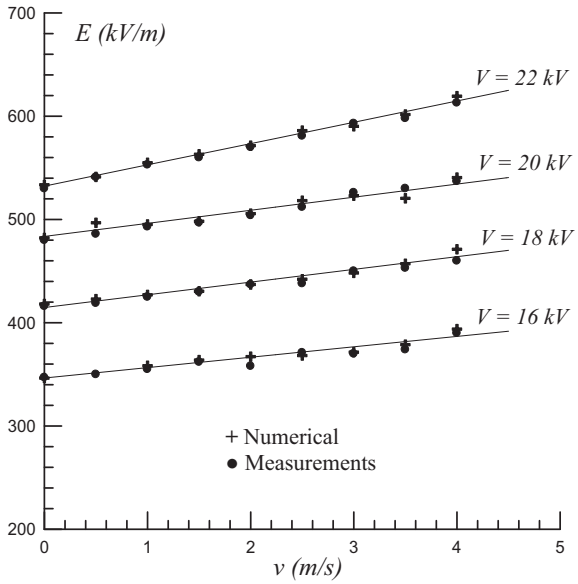

Fig. 7. Electric field at the proximity of the plane surface centre versus the air flow velocity for various applied corona voltage (corona wires radius $R = 0.200$ mm).

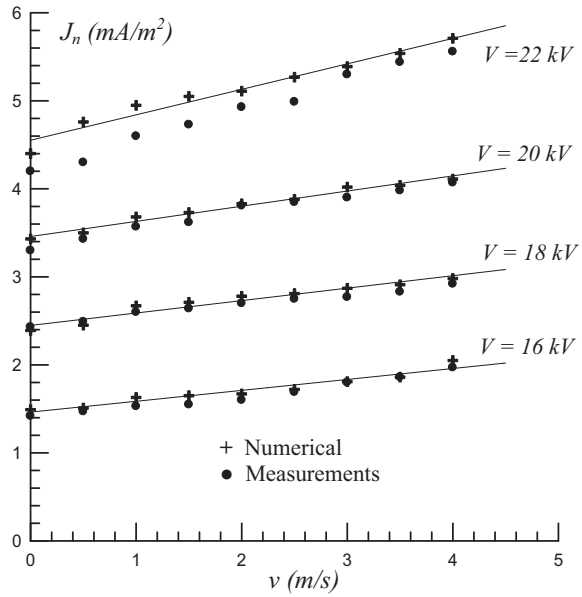

Fig. 8. Normal current density at the proximity of the plane surface centre versus the air flow velocity for various applied corona voltage (corona wires radius $R = 0.200$ mm).

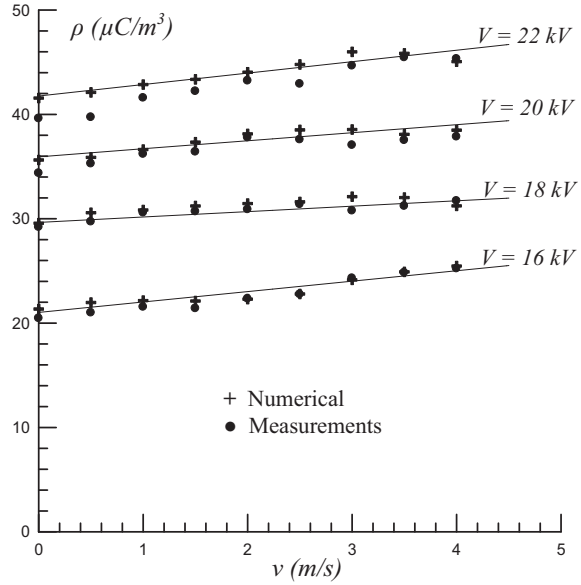

Fig. 9. Space charge density at the proximity of the plane surface centre versus the air flow velocity for various applied corona voltage (corona wires radius $R = 0.200$ mm).

The method of analysis described in this work predicts also the distributions of the electric potential and the electric field in the computed domain and the results are shown in Figures 10 and 11 respectively. It can be seen that the electric potential and the electric field values are higher and the distributions are strongly decreasing near the corona wires (in the ionisation region) and near the collecting planes the values are lower and the distributions are slightly decreasing.

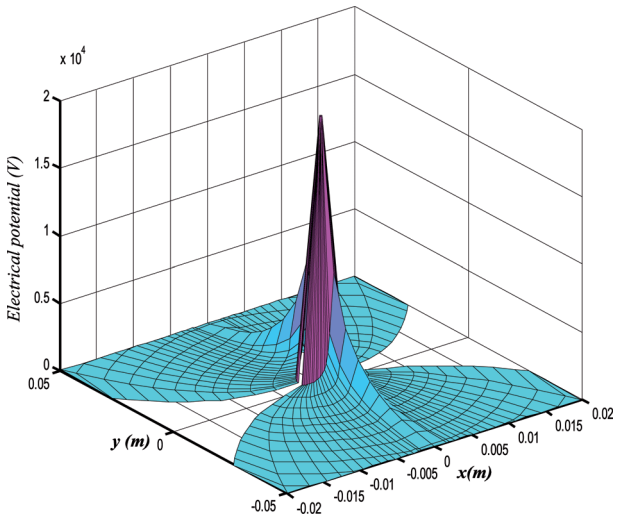

Fig. 10. (Color online) 2D electric potential distribution in the computation domain (corona wires radius $R = 0.200$ mm, applied voltage $V = 20$ kV, air flow velocity $v = 0$ m/s).

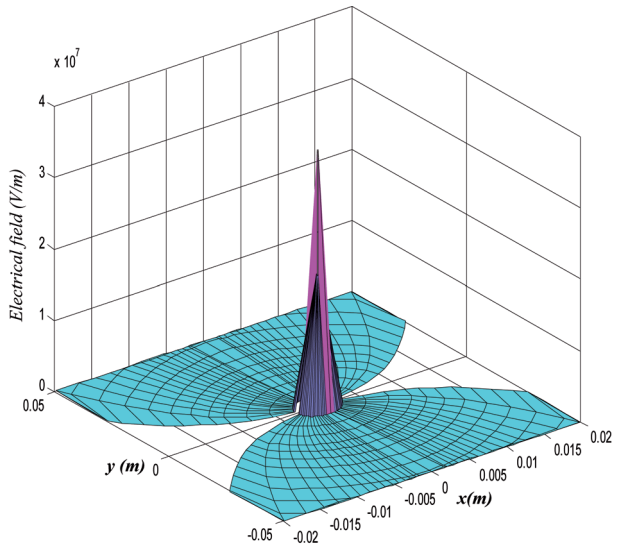

Fig. 11. (Color online) 2D electric field distribution in the computation domain (corona wires radius $R = 0.200$ mm, applied voltage $V = 20$ kV, air flow velocity $v = 0$ m/s)

5 Conclusion

In this paper, an improved efficient iterative method to solve the coupled space charge-electric field problem in the wire to plate electrostatic precipitator system is described. This method uses new boundary conditions which take into account the layer thickness of the ionisation region, whereas in previous works this region is disregarded. The border corresponding to the minimum ionisation field is the third boundary condition introduced which reduces the flow-chart since it eliminates the loop of convergence for the electric field at this border.

Measurements of current density and electric field have been carried out with a good accuracy at the planes surface with the circular biased probe where the measurement

of the air flow velocity, free of all particles, is associated. The presented results indicate a good agreement between numerical and experimental values for the electric field, the current density and the space charge density distributions.

The results of numerical and experiments show that the method is reliable when applied to wire-to-plate electrostatic precipitator taking into account the velocity of the air flow and with neglecting the turbulence due to the electric wind. Future work will use these results to determine the performances of electrostatic precipitators and their efficiency when pollution particles are combined with the air flow.

References

1. G. Cooperman, IEEE Trans. Ind. Appl. **17**, 236 (1981)
2. O.J. Tassicker, IEE Proc. SMT **21**, 213 (1974)
3. E.O. Selim, R.T. Waters, IEEE Trans. Ind. Appl. **16**, 458 (1980)
4. Y. Zebboudj, Ph.D. thesis, Université Paris 6, 1988
5. Y. Zebboudj, IEE Proc. SMT **147**, 74 (2000)
6. D.A. Spence, Proc. Cambridge Phil. Soc. **68**, 529 (1970)
7. Y. Zebboudj, R. Iken, Eur. Phys. J. Appl. Phys. **10**, 211 (2000)
8. K. Adamiak, IEEE Trans. Ind. Appl. **30**, 387 (1994)
9. J.L. Davis, J.P. Hoburg, *Wire-Duct Precipitator field and charge computation using finite element and characteristics methods* (Elsevier Science Publishers B.V., 1983)
10. M. Abdel-Salam, Z. Al-Hamouz, IEE Proc. SMT **141**, 369 (1994)
11. A.J. Medelin, R. Morrow, C.A.J. Fletche, J. Electrostat. **43**, 61 (1998)
12. W. Deutsch, Ann. Phys. Lpz. **16**, 588 (1933)
13. N.A. Kaptzov, OGIZ Moscow (URSS), 587 (1947)
14. G. Hartmann, IEEE Trans. Ind. Appl. **20**, (1984)
15. M. Abdel-Salam, D. Witanen, IEEE Trans. Ind. Appl. **38**, 274 (1993)
16. Z.M. Al-Hamouz, IEEE Trans. Ind. Appl. **38**, 43 (2002)
17. Y. Zebboudj, G. Hartmann, Eur. Phys. J. Appl. Phys. **7**, 167 (1999)